American Mineralogist, Volume 83, pages 1077–1082, 1998

Oriented attachment and growth, twinning, polytypism, and formation of metastable phases: Insights from nanocrystalline TiO_2

R. Lee Penn[1] and Jillian F. Banfield[1,2,*]

[1]Materials Science Program, University of Wisconsin-Madison, Madison, Wisconsin 53706
[2]Mineralogical Institute, University of Tokyo, Hongo, Bunkyo-ku, Tokyo 113, Japan

Abstract

Atomic-resolution transmission electron micrographs show that nanocrystalline TiO_2 coarsens by oriented attachment and growth under hydrothermal conditions. In addition to forming homogeneous single crystals, attachment at anatase surfaces leads to twinning on {112} and intergrowths on (001) and {001}. Brookite, a polytype of anatase, occurs at some {112} twin surfaces. Alternating two octahedra-wide structural slabs in brookite are shared with the two adjacent anatase twin domains. Because {112} anatase twin interfaces contain one unit cell of brookite, we propose that brookite may nucleate at twin planes and grow at the expense of anatase. Alternatively, anatase-brookite interfaces may form by oriented attachment of primary brookite and anatase {112} crystallites. In this case, three unit cell-wide lamellae of brookite are interpreted as remnants of larger crystals that partly converted to anatase by propagation of the anatase-brookite interface. Which phase is stable is unclear over this particle size range, and products of random thermal fluctuations may be preserved by quenching. Regardless of reaction direction, polytypic interconversion of anatase and brookite essentially involves displacement of Ti (by **c**/4 brookite) into adjacent octahedral sites in one of the pair of two octahedra-wide structural slabs. The results have broad relevance for nucleation and growth models as they suggest that twinning and polytypism in macroscopic crystals can originate at oriented interfaces between primary nanocrystalline particles early in their crystallization history.

Introduction

Mechanisms of phase transformations, reasons for nucleation of materials considered to be metastable phases, origin of twinning, and explanations for the development of polytypic intergrowths are fundamental questions with relevance across all disciplines involving the solid state. Phase stability may depend upon surface energy differences between polymorphs, so that phase relationships and transformation kinetics may be dramatically modified when particles are small (Banfield et al. 1993; Gribb and Banfield 1997; McHale et al. 1997; Zhang and Banfield 1998). Understanding the relationships between crystal size, crystal morphology, and stability is central to determining the primary mechanisms controlling crystallization. Twinning, stacking faults, and polytypic intergrowths observed frequently in natural and synthetic crystals can originate during nucleation and early growth, or can result from phase transitions or deformation. The early crystallization history is crucial to understanding phase stability and development of some microstructures; therefore, theoretical, experimental, and crystallographic analysis of natural and synthetic particles in the <15 nm range is extremely important.

In this paper, we show that a coarsening mechanism involving oriented attachment followed by growth can directly lead to the formation of defects and intergrowths. Oriented attachment occurs when particles join at specific dimensionally similar crystallographic surfaces. Furthermore, we show that twin interfaces that contain structural elements not present in bulk materials may play an important role in the nucleation of new phases. The nanocrystalline TiO_2 system examined here provides some insights into the kinetics of more general processes in finely crystalline materials.

Experimental methods

The research was conducted using anatase and brookite, TiO_2 polymorphs, consisting of octahedrally coordinated Ti^{4+} ions. This material is ideal for the study of phase transformation kinetics and the behavior of nanocrystalline materials because it is easy to synthesize, it lacks structural water, and the 4+ oxidation state of Ti is stable under most experimental conditions.

Anatase used in this study was synthesized via the sol gel route described elsewhere (Gribb and Banfield 1997; Bischoff 1992). Following synthesis, anatase sols were dialysized using a Spectra/Por (MWCO = 2000) membrane with deionized water (changed 11 times) to remove the byproducts of synthesis. Prior to dialysis, sols of anatase had not gelled and had low viscosity (similar to that

* E-mail: jill@geology.wisc.edu

0003–004X/98/0910–1077$05.00

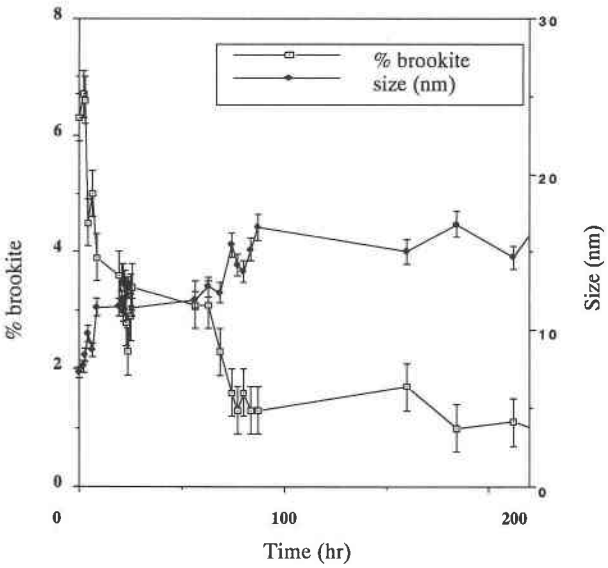

FIGURE 1. Plot of brookite particle size and content (weight percent) vs. hydrothermal treatment time (250 °C). Error bars were determined by statistical analysis of four repetitions of diffraction data from the same sample.

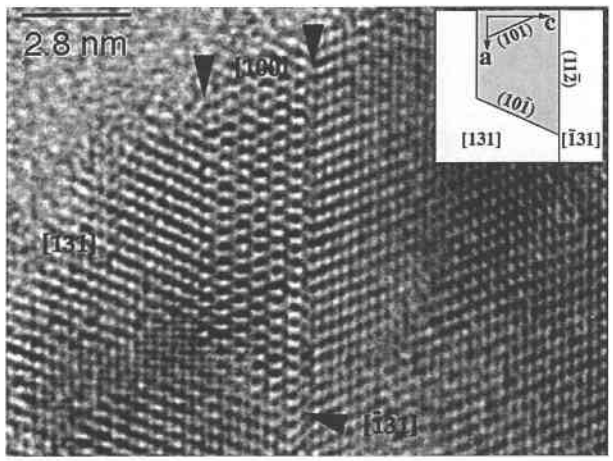

FIGURE 2. HRTEM image of a particle containing anatase intergrown in three orientations. Boundaries are indicated by arrows and represented schematically in inset.

of water). Following dialysis, the sols had gelled, indicating that the pH had risen to near the isoelectric point of anatase [measured pH ~5.5, coinciding with the isoelectric point range reported by Bischoff (1992)].

Several drops of undiluted sol were placed on a randomly cut and polished slab of quartz for X-ray diffraction (XRD) analysis using the Scintag Pad V 4-axis X-ray diffractometer. Anatase particle size was determined along [101] and [001] using the Scherer equation. The average particle size of anatase was measured normal to {101} and of brookite was measured normal to {121} before and after hydrothermal treatment.

Suspensions (~3 mg anatase/g sol) were placed in the Teflon cups of Parr Instrument (model 4744) general purpose acid digestion vessel and placed in a furnace held at temperatures ranging from 100 to 250 °C for times ranging from 1 to 255 h. After the experiments, the vessels were removed and allowed to cool to room temperature.

Samples were prepared for high-resolution transmission electron microscopy (HRTEM) by dispersing particles onto carbon coated Formvar support films on copper grids. Samples were examined in a Philips CM200UT transmission electron microscope (TEM) C_s = ~0.5 mm). Atomic-resolution images were simulated using the EMS software (Stadelmann 1992).

RESULTS

Scherer analysis of broadening of the {101} anatase peak showed that the average anatase particle size of our samples ranged from 5 nm (initial starting material) to 17 nm (coarsest material produced from the 5 nm starting material in hydrothermal experiments). Quantitative XRD results show the starting material contains 6.4% ± 0.4% (as determined by four repetitions) brookite with an average particle size of 8 nm. After 184 h at 250 °C, samples contain 1% ± 0.4% brookite with an average particle size of 17 nm (Fig. 1). By the time the abundance of brookite approaches the detection limit, the remaining crystals have coarsened to an average diameter of about 27 nm. Details of anatase growth and evolution of morphology will be reported elsewhere.

TEM characterization shows the particles in the starting material are free of defects and intergrowths. A particle from a sample hydrothermally treated at 250 °C for 71.75 h (Fig. 2) consists of an intergrowth of a three unit cell wide slab of anatase viewed down ⟨100⟩ (center top) at an interface between two anatase crystals viewed down ⟨131⟩ (bottom left and right). Anatase viewed down ⟨131⟩ occurs in two twin related orientations (see inset diagram). The vertical twin plane between the ⟨131⟩ anatase crystals is {112}. The two other interfaces separating the three unit cell wide strip of [100] anatase from surrounding ⟨131⟩ brookite in Figure 2 involve (001)//{11$\bar{2}$} and {101}//{10$\bar{1}$} (see inset diagram). Reflections from anatase [100] superimpose almost exactly on reflections from the reciprocal lattices of twinned anatase viewed down ⟨131⟩.

Brookite lamellae are present at some planar interfaces (Figs. 3, 4, 5) in hydrothermally treated samples. Brookite (100) is parallel to anatase {112} with brookite [01$\bar{1}$] parallel to anatase ⟨131⟩. The wider of the two brookite slabs bounded by twinned anatase (hydrothermally treated at 250 °C for 117.8 h) in Figure 3a is 11 nm wide and the brookite slab in Figure 3b (hydrothermally treated at 250 °C for 71.75 h) is three unit cells wide.

Figure 4a shows brookite in a sample hydrothermally treated at 250 °C for 117.8 h, viewed down [1$\bar{1}$0] anatase. Brookite occurs in two oriented nanocrystals ("1") viewed down [010] and joined on brookite (100) [see inset rotationally filtered (Kilaas 1997) image of the in-

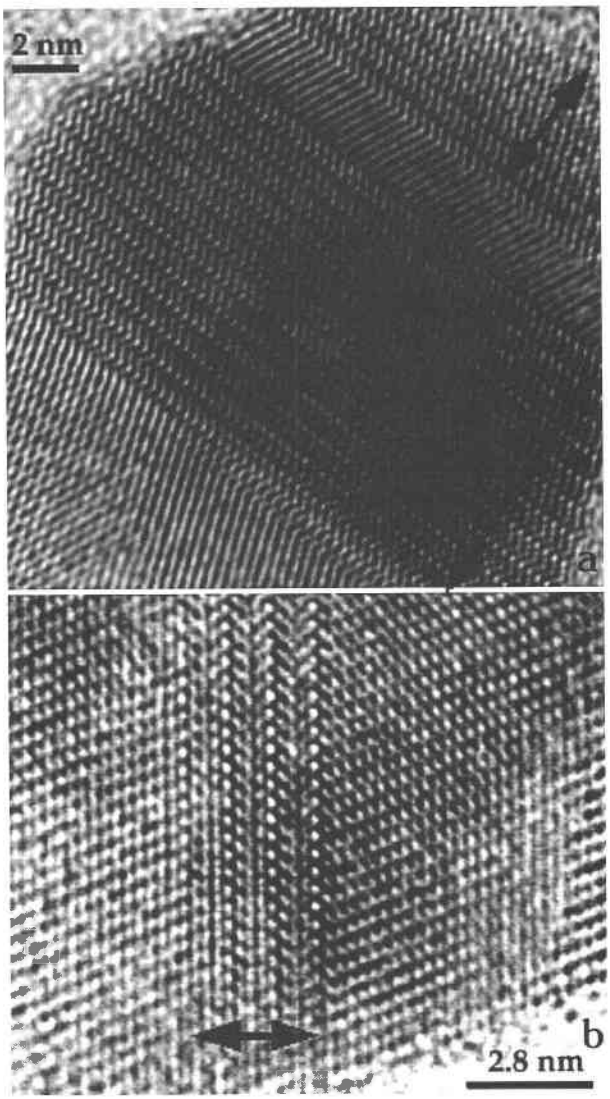

FIGURE 3. HRTEM images of anatase viewed down [131] and brookite down [011]. The boundary is anatase and (100) brookite. (**a**) domains of brookite (indicated by arrows) separated by anatase in twinned orientation; (**b**) three unit cell-wide strip of brookite in anatase.

terface]. Brookite in area "2" (intergrown with anatase in the lower right of Fig. 4a) is viewed down [$1\bar{1}0$] [see reflections in the power spectrum (Fourier transforms; FFTs) in Fig. 4b]. Figure 4c shows the relationships between the anatase and two brookite reciprocal lattices. Three symmetrically equivalent {112} anatase planes are indicated. Note that ($1\bar{1}2$) anatase (shown by gray arrow, inclined at 60° to 004*) is parallel to (100) brookite (inclined at 59.3° to 110*). Thus, both interfaces between anatase and brookite involve {112} anatase and (200) brookite.

Figure 5a shows an atomic-resolution image of an area of anatase [100], [$1\bar{3}1$], and brookite [011] and associated power spectra from a sample hydrothermally treated at

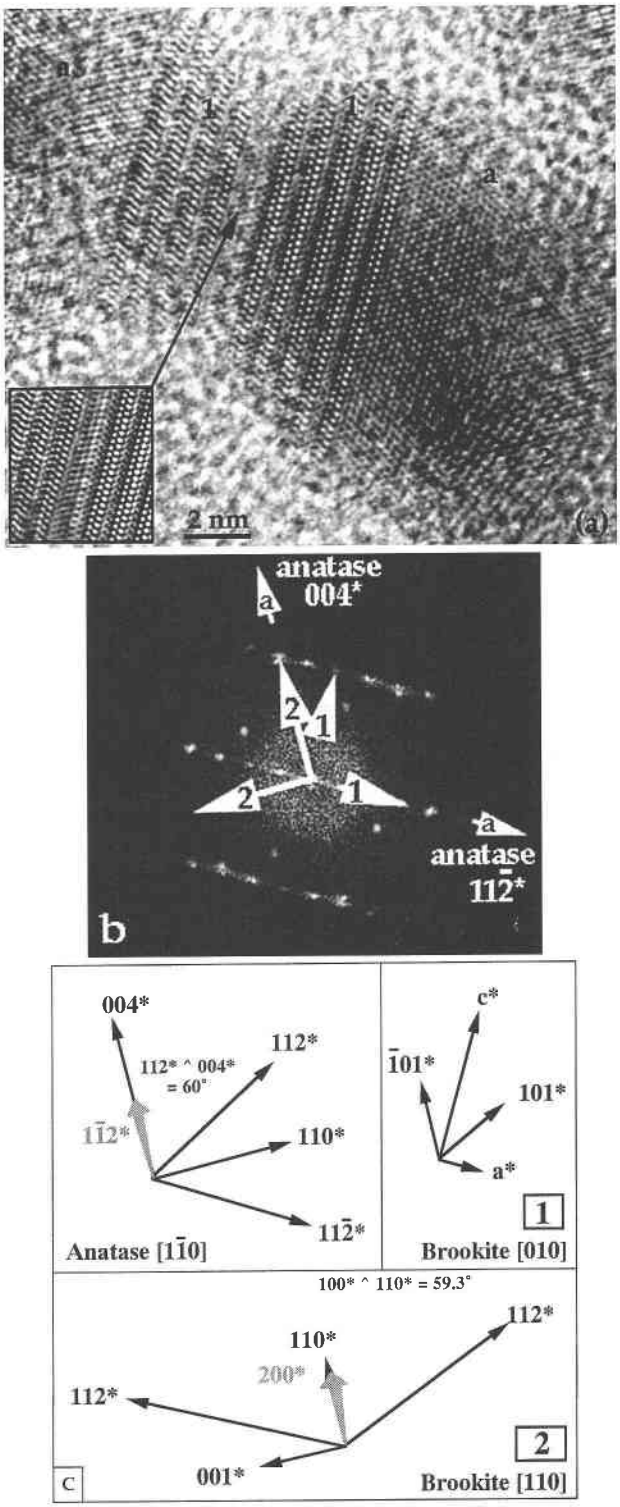

FIGURE 4. (**a**) HRTEM images of particles viewed down [110] anatase. Brookite in orientation "1" is viewed down [010] and "2" down [$1\bar{1}0$]. Inset shows the rotationally filtered contact region (probably brookite). (**b**) FFT of the area in (**a**). (**c**) diagrams of the reciprocal lattices (from anatase "a" and brookite "1" and "2"). Note that brookite "2" also has (200) parallel to anatase {$1\bar{1}2$}.

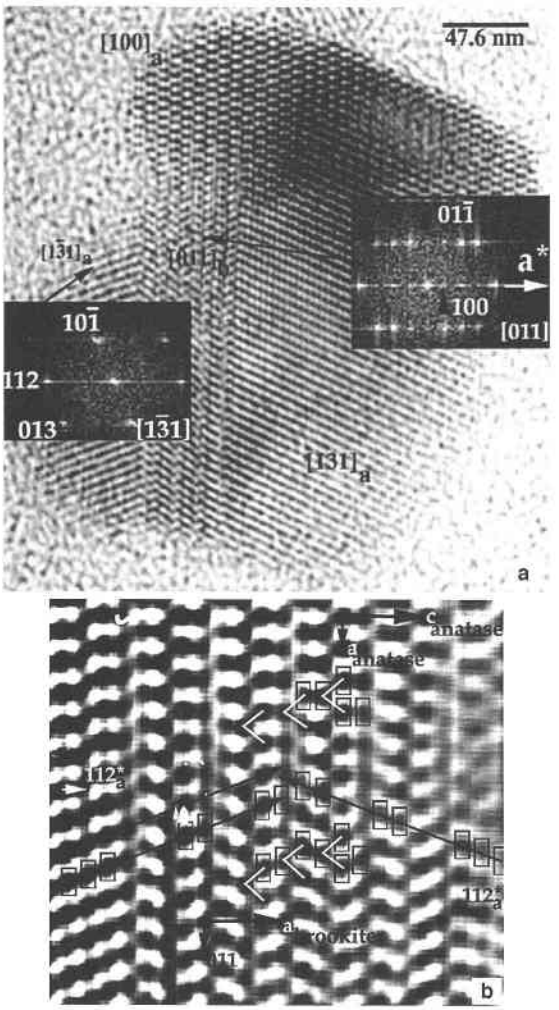

FIGURE 5. (**a**) HRTEM image of a particle containing brookite (vertical strip) at the interface between twinned anatase crystals (lower left and right) and a region of anatase viewed down [100] (top). FFTs are shown as inset. (**b**) rotationally filtered enlarged region from (**a**) with atomic resolution. See text for further explanation.

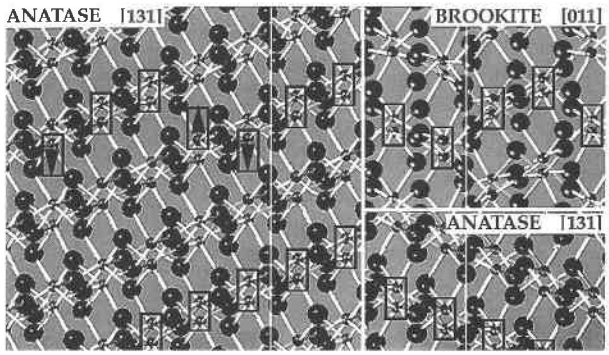

FIGURE 6. Diagram of an anatase-brookite interface (top) and an anatase-anatase twin surface (bottom) viewed down [131] anatase and [011] brookite. Boxes indicate columns of Ti atoms and boxes with arrows indicate Ti positions in brookite (and displacements needed for anatase → brookite). The four rows of octahedra at the anatase twin plane comprise one unit cell of brookite.

250 °C for 71.5 h. The pattern of dark spots toward the top of the rotationally filtered (Kilaas 1997) enlargement (Fig. 5b) corresponds to the Ti atom distribution in anatase viewed down [100]. The pattern of black spots below corresponds to Ti positions in brookite [011], whereas patterns in regions to the left and right of brookite correspond to the Ti distribution in twin related ⟨131⟩ orientations (confirmed by simulations for images recorded close to Scherzer defocus, specimen thickness = 5–10 nm). Note that the pattern in brookite involves two slabs, each consisting of two (vertical) columns of Ti cations (imaged as dark spots). The first of the slabs is common to [131] anatase to the right of [011] brookite, and the second is common to anatase [$1\bar{3}1$] on the left (see black arrows linking boxes marking Ti column positions in anatase and brookite). Furthermore, a slab consisting of one column of Ti from each of these is continuous with the [100] anatase above (see white "<" in Fig. 5b).

Figure 6 illustrates the atomic structure of an anatase-brookite interface (vertical boundary, top right) and a anatase twin boundary (vertical boundary, bottom right). The crystal orientations and interface arrangements shown in this figure are as observed in Figure 5. Brookite can be created from anatase (or vise versa) by displacing Ti atoms into adjacent octahedral sites along two of the four (vertical) {112} planes (see arrows; black boxes indicate the position of cation pairs after cation displacement. Note that the arrangement of black boxes after displacement in anatase is the same as in brookite).

The {112} anatase twin plane structure viewed down ⟨131⟩ (lower right side of Fig. 6) involves a rotation of the structure by 180° around [112]*. Note the displacement necessary to recreate the O plane at the twin surface. This displacement can be observed between {101} lattice fringes either side of the interface in Figure 2 and can be inferred by extrapolation through undisplaced slabs in brookite (black arrows in Fig. 5b). Vertical white lines show that twin region consists of one unit cell of brookite.

DISCUSSION

Banfield and Veblen (1992) showed that brookite can be considered as a polytype of anatase, constructed from essentially identical octahedral layers stacked in different ways (anatase: − − − − vs. brookite: + + − −, where + and − refer to the octahedral tilts; Fig. 7). In view of the above results (Fig. 6), we propose a solid state anatase ↔ brookite transformation mechanism involving displacement of Ti. Note that displacements rotate the octahedral tilts (e.g., + becomes −; Fig. 7). If the direction of the reaction is brookite → anatase, displacements are 0, 0, + **c**/4, − **c**/4 brookite.

In hydrothermally coarsened samples, brookite is typically associated with anatase twin planes and particle

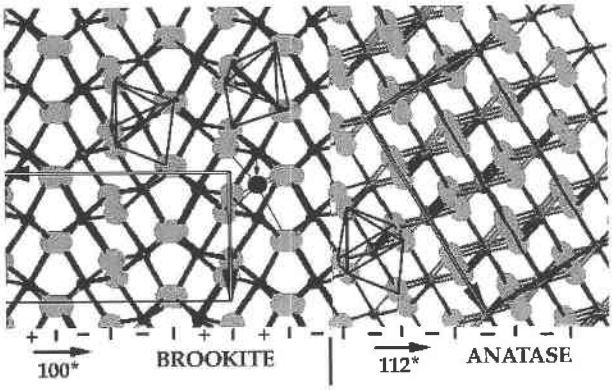

FIGURE 7. Diagram of an anatase-brookite interface down [010] brookite and [110] anatase. The black arrow and black circle show the displacement of Ti needed to convert the next slab of brookite to anatase (rotating the octahedra).

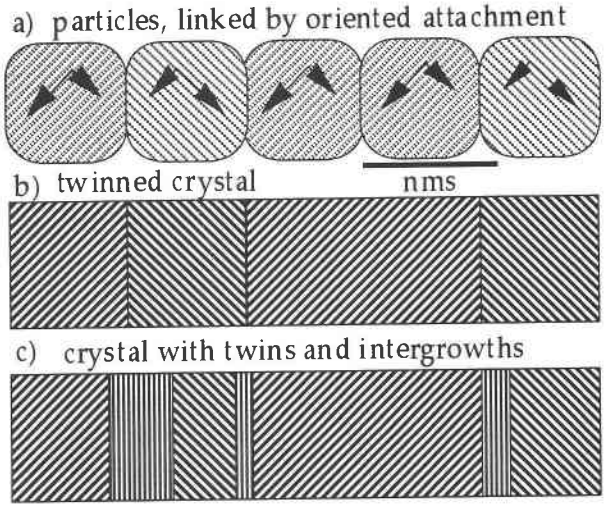

FIGURE 8. Diagram showing oriented attachment of primary particles at a specific surface (**a**), leading to formation of twinned crystals (**b**), and, if a new phase nucleates at twin surfaces, twinned and intergrown crystals (**c**).

contacts (Fig. 4a). The increase in brookite size compared to the starting material (Figs. 1 and 3a) and change in morphology (from almost spherical particles to more elongate lamellae with planar boundaries) indicate growth during hydrothermal treatment. However, some brookite laths are considerably narrower than the primary particles (e.g., Fig. 3b) and Figure 1 indicates an overall decrease in brookite abundance with time. Thus, our data suggest metastable crystallization of brookite in parallel with brookite dissolution or transformation to anatase. The persistence of a few larger crystals of brookite into the sub-micrometer to micrometer size range is expected. This is consistent with the presence of macroscopic brookite in some natural samples.

Change in brookite size and morphology may involve a combination of three processes: (1) brookite and anatase particles attach in an oriented way and brookite coarsens by addition of atoms from solution or by transformation from anatase, (2) brookite sandwiched by oriented anatase particles is partly (and ultimately, completely) consumed by conversion to anatase, and (3) brookite forms at anatase twin surfaces. Evidence for both growth and reduction in brookite dimensions implies both (1) and (2) occur. The transformation mechanism described above (Figs. 6 and 7) is probably important for (2) and may be involved in (1).

It may be tempting to rule out (3), based on known phase relationships. For example, calculations by Post and Burnham (1986) indicated that macroscopic brookite is metastable with respect to both anatase and rutile, suggesting that brookite should transform either to anatase or rutile. However, surface energy can significantly modify phase relationships when the particle size is very small (e.g., Langmuir 1971; Banfield et al. 1993; Gribb and Banfield 1997; McHale et al. 1997; Zhang and Banfield 1998). Specifically for TiO_2, it has been argued from both experimental and theoretical standpoints that anatase may be stabilized relative to rutile at small particle size due to its lower surface energy (Banfield et al. 1994; Gribb and Banfield 1997; Zhang and Banfield 1998). The lower density of brookite compared to anatase suggests a lower surface energy compared to anatase, but a detailed analysis has not been attempted. Adsorption of ions onto surfaces and lattice strain can further modify phase relations through their effect on surface energy. Under conditions where their structure energies are similar, random thermal fluctuations may drive growth of brookite from anatase. Given the particle size effects on phase relationships and the small volumes of material involved (probably not greatly exceeding the critical size), formation of brookite from anatase by a solid state reaction is possible.

Nucleation of brookite may be promoted by the fact that {112} twin surfaces contain a unit cell of brookite (Figs. 6 and 7). This surface can act as a nucleus, and may grow as a stable or nearly stable phase, driven by random fluctuations (which can be quenched in) or a thermodynamically driven phase transformation. Assuming the twin surface is energetically unfavorable, this may be a mechanism by which twinned crystals are replaced by homogeneous single crystals. The activation barrier for the transformation is the energy needed to displace octahedral cations into adjacent sites within a structure otherwise only slightly modified by distortion.

An important conclusion from this study is the general result that oriented attachment and growth can lead to formation of planar defects, including twin planes and other interfaces (summarized in Figs. 8a and 8b). These microstructures are a direct consequence of a coarsening mechanism that involves surface tension reduction by elimination of surfaces by attachment that is constrained only in the two dimensions of the interface. In some cases, attachment can lead to formation of twin planes or other interfaces with structures distinct from that of the bulk. These structurally different regions may serve as

nucleation sites for new phases. Complex intergrowths (commonly reported in TEM studies of natural materials, especially layer silicates) may result from sequential oriented attachment (leading to separations between stacking reversals of greater than, or equal to, the primary particle size; Fig. 8b) or finer scale intergrowths if growth occurs from twin surfaces (Fig. 8c). Although our results are experimental, we suggest that coarsening by oriented attachment may be important in nature and explain formation of defects and intergrowths in a variety of minerals.

Acknowledgments

Financial support from The National Science Foundation (Grant no. EAR-9508171), the National Physical Science Consortium (fellowship to R. Lee Penn), and the Mineralogical Society of America (Student Research Award to R.L.P.). Hengzhong Zhang is thanked for helpful discussion. The manuscript was improved by comments from Michael Carpenter, Adrian Brearley, and an anonymous reviewer.

References cited

Banfield, J.F. and Veblen, D.R. (1992) Conversion of perovskite to anatase and TiO_2(B): A TEM study and the use of fundamental building blocks for understanding relationships among the TiO_2 minerals. American Mineralogist, 77, 545–557.

Banfield, J.F., Bischoff, B.L., and Anderson, M.A. (1993) TiO_2 accessory minerals: coarsening, and transformation kinetics in pure and doped synthetic nanocrystalline materials. Chemical Geology, 110, 211–231.

Bischoff, B.L. (1992) Thermal stabilization of anatase (TiO_2) membranes. Ph.D. thesis, University of Wisconsin, Madison, Wisconsin.

Gribb, A.A. and Banfield, J.F. (1997) Particle size effects on transformation kinetics and phase stability in nanocrystalline TiO_2. American Mineralogist, 82, 717–728.

Kilaas, R. (1997) Optimal and near-optimal filters in high resolution electron microscopy. Journal of Microscopy, 190, 45–51.

Langmuir, D. (1971) Particle size effect on the reaction goethite = hematite + water. American Journal of Science, 271, 147–156.

McHale, J.M., Auroux, A., Perrotta, A.J., and Navrotsky, A. (1997) Surface energies and thermodynamic phase stability in nanocrystalline aluminas. Science, 277, 788–791.

Post, J.E. and Burnham, C.W. (1986) Ionic modeling of mineral structures and energies in the electron gas approximation: TiO_2 polymorphs, quartz, forsterite, diopside. American Mineralogist, 71, 142–150.

Stadelmann, P. (1992) Simulation of HREM images and 2D CBED patterns using EMS software package. Software manual 12M-EPFL, Lausanne, Switzerland.

Zhang, H. and Banfield, J.F. (1998) Phase stability in the nanocrystalline TiO_2 system. In E. Ma, P. Bellon, M. Atzmon, R. Trivedi, Eds., Phase Transformations and Systems Driven Far from Equilibrium. Materials Research Society Journal, in press.

Manuscript received September 29, 1997
Manuscript accepted April 27, 1998
Paper handled by A.J. Brearley